FINITE ELEMENT MODELLING OF ELECTRIC CURRENTS IN AC SUBMERGED ARC FURNACES

I. Mc Dougall

CSIR, P. O. Box 395, Pretoria, 0001, South Africa
E-mail: imcdougall@csir.co.za

ABSTRACT

F*inite element models were generated of two submerged arc furnaces of different geometries. A 48MW circular furnace and a 68MW 6-in-line rectangular furnace were studied. The electrodes, raw material, slag and molten metal were included in the model. ANSYS/Multiphysics was used to predict the current density distribution in the electrodes, raw material, slag and molten metal as a result of the three phase AC current. The effect of the electrode immersion on the current path was studied.*

The "proximity effect" caused a pronounced asymmetry in the electrode currents in the circular furnace, whilst the electrode currents in the rectangular furnace exhibited radial symmetry. The current distribution in the melt in both furnaces indicated that the bulk of the current flows between phases. The current density is greatest between electrodes.

Results were compared to qualitatively similar published work, operating experience and results of furnace dig-outs.

1. INTRODUCTION

The distribution of the electric current in a submerged arc furnace is of interest because the electric current is the means by which energy is generated in the form of heat in the system. The baking of the Søderberg electrodes used in these furnaces is affected by the current distribution, as is the position and size of the reaction zone. It is generally accepted that the presence of the electrodes in proximity to each other causes asymmetry of the current distribution as well as the magnetic fields in each electrode.

Bermudez et al. [1] modelled a horizontal slice taken through the three Persson-type electrodes of a round furnace. A quasi-static state was assumed, as the slipping of the electrode was included in the formulation. The model did not include the furnace contents. The asymmetry of current distribution in the electrodes as a result of the presence of neighbouring electrodes, the "proximity effect", was demonstrated in their results.

Dhainaut [2] computed the current path from the electrodes through the furnace contents of a round furnace using the CFD package FLUENT. The AC current was analysed at a single time point. The charge was divided into horizontal layers, each of which had constant material properties.

Sheng, Irons and Tisdale [3] calculated electric current distribution, temperature and flow patterns in a segment of a six-in-line rectangular nickel furnace. In addition, they measured voltage drops in the slag [4]. They found that there was a substantial voltage drop, of the order of 100V, between the electrode and the slag, which they attributed to the presence of an arc which gives rise to a plasma layer around the electrode.

In the present work, finite element models were generated of two submerged arc furnaces of different geometries. The first was a 48MW circular furnace used for the production of ferrochrome, whilst the second was a 68MW 6-in-line rectangular furnace used for the smelting of copper-nickel concentrate. The purpose of the study was to determine the current density distribution in the electrodes, raw material, slag and molten

metal as a result of the three phase AC current. The asymmetry caused by the proximity of the electrodes to one another was of particular interest. The effect of the electrode immersion depth on the current path was also studied. As the objective of this study is to compare the differences in current distribution as a result of the geometry in a semi-qualitative manner, the mere fact of differences in operating conditions caused by the process and the power ratings is not a hindrance.

2. MATHEMATICAL FORMULATION

As the frequency of the current is low, the quasi-static form of Maxwell's equations is solved.

$$\nabla \times \mathbf{E} = -\frac{\partial \mathbf{B}}{\partial t} \tag{1}$$

$$\nabla \times \mathbf{H} = \mathbf{J} \tag{2}$$

$$\nabla \cdot \mathbf{D} = \rho \tag{3}$$

$$\nabla \cdot \mathbf{B} = 0 \tag{4}$$

where **E** denotes the electric field intensity, **H** the magnetic field intensity, **D** the electric flux density, **B** the magnetic flux density, **J** electric current density and ρ the electric charge density.

A harmonic electromagnetic analysis describes the steady state reached when a system is excited sinusoidally. The physical, time-varying field for a variable, q(**r**,t), such as **B**, **H**, **E**, **J**, the vector potential **A** or the scalar potential V, and which depends on space, **r**, and time, *t*, may be expressed as the real part of the complex function

$$q(\mathbf{r},t) = \mathrm{Re}\left\{ Q(\mathbf{r}) e^{j\omega t} \right\} \tag{5}$$

This may be written as

$$q(\mathbf{r},t) = Q_r(\mathbf{r})\cos(\omega t) - Q_i(\mathbf{r})\sin(\omega t) \tag{6}$$

where $Q_r(\mathbf{r})$ and $Q_i(\mathbf{r})$ are the real and imaginary parts of the complex function Q(**r**) and ω is the angular frequency. In ANSYS, the harmonic analysis provides solutions to the real and imaginary components of the complex solution. The phase reference is established in such a way that the magnitude of the real solution describes the measurable field at $\omega t = 0$, whilst the magnitude of the imaginary solution describes the measurable field at $\omega t = -90°$.

3. GEOMETRY OF THE MODELS

The important dimensions of the two furnaces are listed in Table 1.

3.1 Round Furnace

The model includes the three electrodes with their contact shoes, the furnace charge, the slag and the molten metal. The steel casing and fins are important for both mechanical integrity and electrical conduction in the

electrode in the region near the contact shoes. Where the temperature of the electrode exceeds approximately 1000°C, the steel oxidises, losing both its electrical and mechanical properties.

Table 1: General Information on the Furnaces

DIMENSION	*ROUND FURNACE*	*RECTANGULAR FURNACE*
Overall Dimensions	Diameter 10.2m	28.7m x 9.6m
Number of Electrodes	3	6
Electrode Diameter	1.55m	1.6m
Electrode Current	110kA	60kA
Power Rating	48MW	68MW
Process	Ferrochrome Reduction	Copper-Nickel Matte Smelting

3.2 Round Furnace

The model includes the three electrodes with their contact shoes, the furnace charge, the slag and the molten metal. The steel casing and fins are important for both mechanical integrity and electrical conduction in the electrode in the region near the contact shoes. Where the temperature of the electrode exceeds approximately 1000°C, the steel oxidises, losing both its electrical and mechanical properties. At some distance above the electrode tip there is no steel left, and all the current is conducted through the carbon. Previous work done by the author on a model of a single Soderberg electrode [5] indicates that the current density near the tip of the electrode is governed by the skin effect rather than the steel. In this model, the electrodes have been simplified by the removal of the casing and fins. The model is depicted in Figure 1.

3.2.1 Material Properties

Constant isotropic material properties are used for all materials. In order to allow for the change of material properties at different temperatures, the electrodes are divided into three sections, which are assigned the material properties of carbon paste at 120°C, 650°C and 1500°C respectively. In a similar manner, the charge is divided into 3 sections, corresponding to the material properties at 563°C, 919°C and 1422°C. The material properties used and the temperatures represented by these properties are summarised in Table 2. Due to the absence of the steel in this model, none of the materials is considered magnetic. The electrical conductivity of the charge was obtained from work done by Urquhart [6]. The air elements between the contact shoes are required to provide the required electrical insulation between the contact shoes.

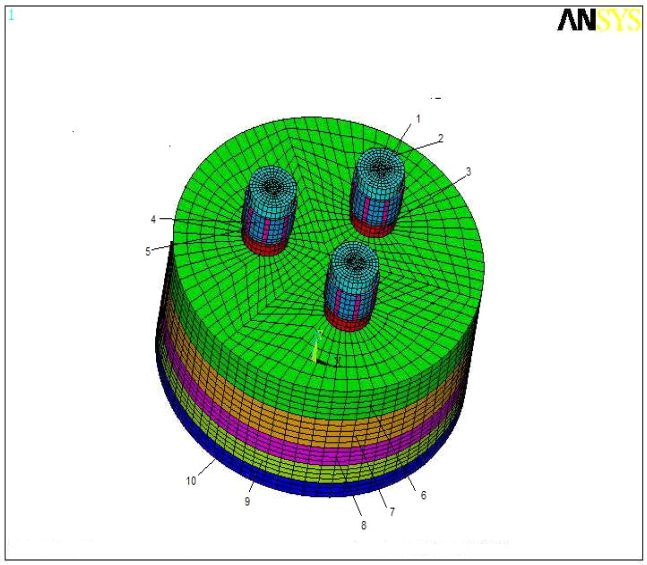

Figure 1: Model of the Round Furnace
The numbers refer to the materials listed in Table 2

Table 2: Material Properties for the Three Electrode Model

Material No. in Figure 1	Material	Temperature	Electrical Resistivity [Ù.m]
1	Electrode Paste	120°C	5.263×10^{-3}
2	Electrode Paste	650°C	0.6024×10^{-3}
3	Electrode Paste	1500°C	0.036×10^{-3}
4	Copper	20°C	0.031×10^{-6}
5	Air	Not temp dependent	3×10^{13}
6	Charge	563°C	2.43
7	Charge	919°C	1.67
8	Charge	1422°C	0.254
9	Slag	1750°C	0.0193
10	Molten Ferrochrome	1750°C	0.61×10^{-6}

3.2.2 Loads and Boundary Conditions

The base of the molten metal is chosen as the voltage reference point, and the voltage is set to zero at this point. This corresponds to the neutral point of the electrode system. The normal component of the magnetic flux density is set to zero on the exterior of the model.

The electrode current is an AC current, at 50Hz, of the form

$$i = \sqrt{2} I_{RMS} \cos\left(\frac{t}{50} - \phi\right) \tag{7}$$

A three phase current is applied to the electrodes, as two phases per electrode. The rotation of the current is clockwise. I_{RMS}=110kA for all the electrodes, and $\varphi = 0°$ and $240°$ for electrode 1, $\varphi = 0°$ and $120°$ for electrode 2 and $\varphi = 120°$ and $240°$ for electrode 3. This represents the actual operating regime in the furnace. A harmonic magnetic analysis is performed in ANSYS at a frequency of 50Hz using the SOLID117 element.

3.3 Rectangular Furnace

A model of the whole furnace was generated. The matte and slag were modelled in detail, as well as the lower 750mm of the electrodes. The furnace lining and externals were omitted. The complete model is shown in Figure 2, whilst a section through the long axis of the model is shown in Figure 3.

3.3.1 Material Properties

A single material property, namely electrical resistivity, is required for each of the three materials. A value of 0.036 Ωm was used for the electrode carbon, as in Table 2. The value used for the slag was 0.033 Ωm, whilst the resistivity of the matte was 10.75×10^{-6} Ωm. These values were obtained from Sheng et al. [3], and apply to a nickel matte and slag.

3.3.2 Loads and Boundary Conditions

The normal operating condition is a Δ connection, with two electrodes per phase. This corresponds to the circuit information used in Sheng et al. [3]. A nominal electrode current of 60kA was used, which corresponds to operation at 68MW and 25% electrode immersion. The electrode current is an AC current, at 50Hz, as in equation (1), where I_{RMS} = 60kA and $\varphi = 0°$ for electrodes 1 and 2, 240° for electrodes 3 and 4 and 120° for electrodes 5 and 6, assuming a clockwise current rotation. This current is applied to the top of each electrode. A voltage of 0V was imposed on the base of the matte, as the matte represents an equipotential plane as a

Figure 2: Rectangular furnace model

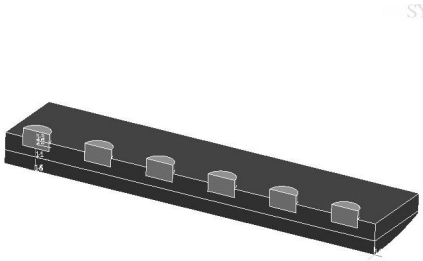

Figure 3: Section through the long axis of the rectangular furnace

result of its low electrical resistivity, and is the neutral point of the Δ connection. A harmonic magnetic analysis at 50Hz was conducted on the model using ANSYS®. The SOLID117 element was employed for this analysis, as this formulation has been shown to be suitable in applications where there are materials of different resistivity. When this formulation is used, it is necessary to set the normal component of the magnetic flux density to zero at the exterior of the model.

4. RESULTS

The current density in the electrodes and furnace contents is the primary variable of interest in this analysis, although voltage drop, magnetic flux density and magnetic field are also calculated.

The skin depth in the lower portion of the electrode may be calculated from the formula

$$\delta = \frac{1}{\sqrt{\pi \mu \sigma f}} \tag{8}$$

where δ is the skin depth in metres, π= 22/7, μ is the permeability of a vacuum, (4 π 10^{-7} Henry per metre), σ is the electrical conductivity in Siemens per metre and f is the frequency in Hertz. For a resistivity of 0.036 x 10^{-3} Ω.m at 50Hz this equates to a skin depth of 427mm. This is approximately 55% of the diameter of the electrodes.

4.1 Round Furnace

Results are presented for where current is applied to the electrodes as two phases per electrode. The current distribution in the electrodes above the charge depicted in Figure 4 exhibits a concentration of current displaced towards the direction of rotation of the phases. The position of the region of maximum current density in each electrode in this plot is in good agreement with results published by Bermudez et al [1].

Figure 5 shows contours of the modulus of current density through the furnace, whilst contours of the current density in the molten metal are shown in Figure 6. Very little current passes through the charge, whilst current passes into the slag in a relatively small region below the electrode. This is consistent with the findings of furnace dig-outs [7], in which isolated reaction zones are observed below the electrodes. The temperature in these reaction zones is hotter than the surrounding material. In an operating furnace, there is some degree of electromagnetic stirring in the slag and molten metal as a result of the magnetic fields, which may increase

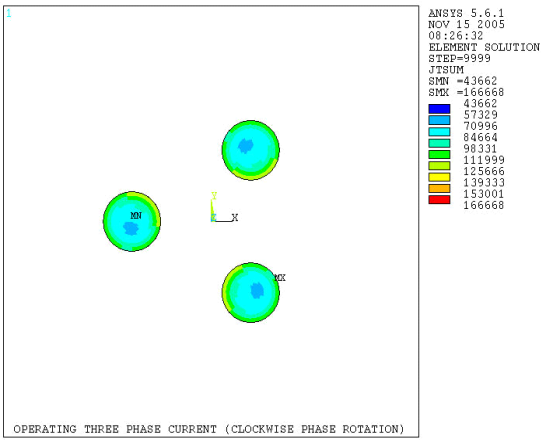

Figure 4: Modulus of current density in the electrodes for a three phase input current

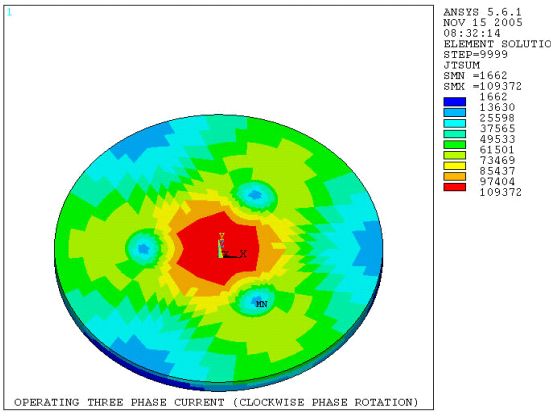

Figure 6: Current density in the molten metal for a three phase current

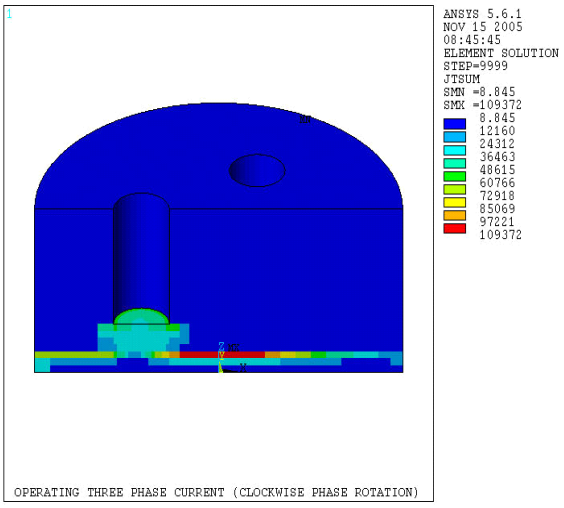

Figure 5: Modulus of current density through th furnace centreline

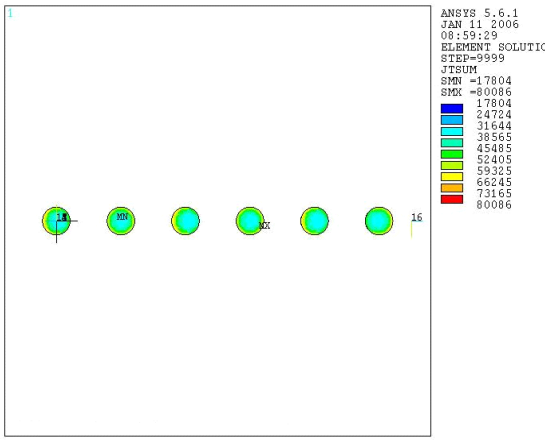

Figure 7: Modulus of current density in the electrodes above the slag

the extent of the reaction zones somewhat. This effect has not been considered in this model. The greater portion of the current in the molten metal is in the centre of the furnace between the electrodes. The spikes in the contours in the current density plots appear to be due to the limitations of the contouring algorithm. The maximum current density in the molten metal is approximately 109 372 A/m^2.

4.2 Rectangular Furnace

The modulus of current density in the electrodes above the slag is shown in Figure 7. Electrode 1 is on the left. The concentration of current towards the surface of the electrodes is apparent. There is a concentration of current on the side of electrode 2 which faces electrode 3, and a corresponding reduction in current where electrode 2 faces electrode 1. This demonstrates the repulsive force between electrodes fed by the same phase, and the attractive force between electrodes fed from different phases. The skin effect is not as well defined as expected, as there appears to be a gradual attenuation of the current density towards the centre of the electrode

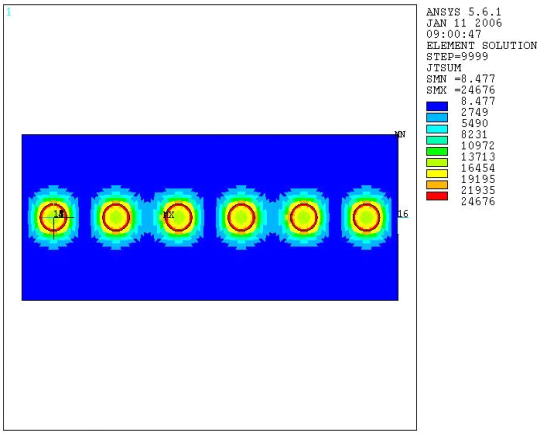

Figure 9: Modulus of current density in the matte

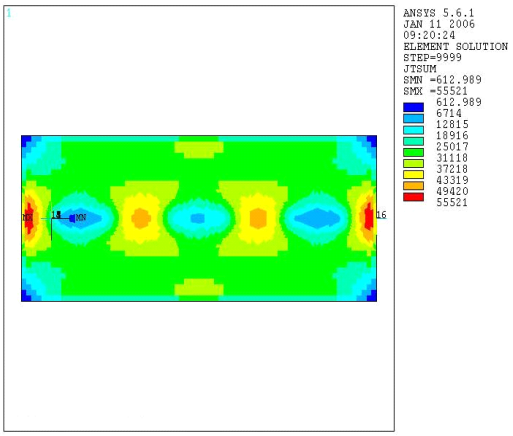

Figure 10: Modulus of current density in a section through the furnace near electrode 5 with brush arcing of electrodes

rather than an abrupt change. The current distributions are symmetric across the furnace centerline, as there is nothing to disturb this symmetry. Current density in the slag is shown in Figure 8, whilst current density in the molten matte is shown in Figure 9. As the resistivity of the slag is several orders of magnitude greater than that of the matte, it follows that the current passes downwards through the slag to the matte without a significant horizontal dissipation, and that very little current flows near the walls. This is consistent with the results for the round furnace. The current path in the matte is concentrated near the top surface. The dominant path is between electrodes 2 and 3, and 4 and 5. The concentration of current at the ends of the furnace in Figure 9 is interesting and bears further investigation.

The effect of the immersion depth of the electrode on current distribution was studied. Electrode penetration into the slag of 25%, 50% and 0% (electrode touching the slag surface) were considered. All other conditions were kept constant. As the resistance of the slag is dependent on the depth of immersion of the electrodes, the power input reduces as the electrode is lowered and the current remains the same. This reduces the resistance heating in the system. Conversely, to maintain the same power input, the electrode current must be increased if the electrode is lowered. The current distribution in the matte is not greatly affected by changes in electrode depth. The current distribution in the slag and electrode does not change appreciably between 25% and 50% immersion if the current is kept constant. This is used to advantage in operating furnaces to fine-tune the power and heat input to the furnace in order to accommodate variations in the slag resistance.

The brush arcing condition (0% penetration) exhibits a very high current density in the slag immediately adjacent to the electrode, as shown in Figure 10. Comparison of Figure 10 with Figure 8 indicates that the peak current density in this region is considerably higher than that for 25% immersion. This effect is fairly localised and likely gives rise to high local temperatures and a rapid reaction rate. A higher proportion of the energy in the slag is dissipated in this region, leading to reduced effectiveness of the reaction in the remainder of the furnace.

5. CONCLUSIONS

The distribution of electric current was calculated by means of finite element models for two reduction furnaces of different geometries. The skin depth was approximately half the radius of the electrodes. The asymmetry in the current distribution in the electrodes due to the proximity of the other electrodes was demonstrated. The current distribution in the molten metal was found to be insensitive to the depth of immersion of the electrode in the slag. The depth of immersion of the electrode affects the resistance of the current path through the slag, and hence the amount of resistive heating occurring in the slag.

REFERENCES

[1] Bermudez, A., Muniz, M.C., Pena, F. , Bullon, J., " Numerical Computation of the Electromagnetic Field in the Electrodes of a Three-Phase Arc Furnace", Int. Jnl for Numerical Methods in Engineering, 1999, Vol 46, pp 649-658.

[2] Dhainaut, M., "Simulation of the Electric Field in a Submerged Arc Furnace" , Proc. INFACON X, pp 605-613, 2004.

[3] Sheng, Y.Y, Irons, G.A., Tisdale, D.G., "Transport Phenomena in Electric Smelting of Nickel Matte: Part 1. Electric Potential Distribution", Metallurgical and Materials Transactions B, Vol 29B, Feb 1998, pp 77-83.

[4] Sheng, Y.Y, Irons, G.A., Tisdale, D.G., "Transport Phenomena in Electric Smelting of Nickel Matte: Part 2. Mathematical Modelling", Metallurgical and Materials Transactions B, Vol 29B, Feb 1998, pp 85-94.

[5] Mc Dougall, I., "Computational Modelling of Søderberg Electrodes", PhD Thesis, University of Wales, Swansea, 2006.

[6] Urquhart, R.C., "A Study of the Production of High-Carbon Ferrochromium in the Submerged-Arc Furnace", PhD Thesis, University of the Witwatersrand, Johannesburg, 1972.

[7] Wedepohl, A., Barcza, N. A., " Observations made during the Dig-Out of a 48MVA Ferrochromium Furnace", National Institute for Metallurgy Report No. 2090, July 1981.